Effect of enhancers and inhibitors on photocatalytic sunlight treatment of dye wastewater

Wennie Subramonian, Ta Yeong Wu*

Chemical Engineering Discipline, School of Engineering, Monash University, Jalan Lagoon Selatan, Bandar Sunway, 46150, Selangor Darul Ehsan, Malaysia.

*Corresponding author: Ta Yeong Wu

E-mail addresses: wu.ta.yeong@monash.edu; tayeong@hotmail.com

Tel: +60 3 55146258

Fax: +60 3 55146207

Abstract

In view of the fatal illnesses which Methylene Blue (MB) leads to upon ingestion, the present study focused on the use of natural sunlight in heterogeneous photocatalysis to decolourize MB. Most past studies utilized UV, visible or simulated sunlight in photocatalysis of MB. The present study also investigated the effects of enhancers (hydrogen peroxide and persulphate ion) and inhibitors (chloride and carbonate ions) on photodecolourization of MB. Pseudo-first-order rate constants for each studied effect were determined through Langmuir-Hinshelwood model. The recommended conditions to photodecolourize 60 ppm of MB under natural sunlight were 1.0 g/L titanium dioxide nanopowder at initial pH 10.5 in order to achieve 85.3% decolourization (rate constant of 10.8 $\times 10^{-3}$ min^{-1}). The addition of 4080 ppm hydrogen peroxide and persulphate ion significantly enhanced the decolourization efficiency up to 96.6 and 99.3%, respectively (rate constants of 66.2 and 91.0×10^{-3} min^{-1}, respectively). However, the addition of 2000 ppm chloride and carbonate ions reduced the decolourization efficiency of MB to 74.7 and 70.2%, respectively (rate constants of 7.8 and 7.3×10^{-3} min^{-1}, respectively). The present study implied that it was possible to use natural sunlight as a light source for photocatalytic treatment of dye in tropical countries like Malaysia.

Key words: carbonate ion; chloride ion; hydrogen peroxide; methylene blue; persulphate ion

Introduction

One of the major pollutants found in water resources discharged around industrial areas is dye and more than one million ton of dyes are produced annually worldwide (Chiu et al., 2010). Treatment of wastewater containing dyes is one of the growing needs of the present time because most dyes with a complex aromatic molecular structure are considered to be non-oxidizable substances by traditional biological and physical treatment (Kumar and Bansal, 2012; Sun et al., 2013). It is estimated that 90% of total dyes produced are used in fabrics whereas the remaining in leather, paper, plastic and chemical industry (Pandg and Abdullah, 2013). In 2011, there were 662 licensed textile and clothing industries in Malaysia, representing a total investment of USD 2.6 billion (Saheed, 2012). However, 15% of the total world production of dyes is lost during the dyeing process and released in textile effluents (Lachheb et al., 2002). In fact, World Bank estimates that 17-20% of industrial water pollution comes from textile dyeing and treatment industries (Chan et al., 2011). The textile wastewater treatment has been considered as one of the most important categories of water-pollution control due to its high colour intensity and high organic contamination (Lee et al., 1999).

The chosen dye in this study was Methylene Blue (MB). MB is a cationic dye which is extensively used in dyeing industry (Saif Ur Rehman and Han, 2013). Advanced Dyestuff and Chemicals Pvt. Ltd. (2011) reported that MB is one of the major dyes imported into Malaysian textile industry, printing industries and occasionally in the medical field. A toxicology test among 7 adult men and found that 26% MB was absorbed by the body from the consumption of a 10 mg MB gelatin capsule (National Toxicology Program, 2013). It was also concluded that acute ingestion of MB led to increasing heart rate, cyanosis, shock, vomiting, quadriplegia, Heinz body formation and tissue necrosis in humans (National Toxicology

Program, 2013). Lodha et al. (2010) further stated that overdose of MB caused nausea, abdominal and precardial pain, dizziness, headache, profuse swelling, sweating and mental confusion.

Conventional dye wastewater treatment methods include physicochemical and biological methods (Álvarez et al., 2013; Wang et al., 2014). According to Wang et al. (2014), these conventional treatment methods for dye wastewater are proven unsatisfactory. Biological methods result in lower decolourization efficiency due to inconsistency in quality and quantity of wastewater discharged (Lee et al., 1999). Also, the use of biological treatment system alone results in the incomplete degradation of recalcitrant compounds (Ghaly et al., 2011). In addition, degradation of dyes under anaerobic conditions produces aromatic amines, which are carcinogenic and more hazardous (Low et al., 2012). Membrane separation suffers from membrane fouling and higher in cost due to regular change of membrane. Chemical methods are still widely favoured and used due to high degradation ability and generation of powerful oxidizing agents but the efficiencies are strongly influenced by the type of oxidant (Forgacs et al., 2004; Kitture et al., 2010).

Recently, degradation of dyes through oxidative methods receives considerable attention because of its ability to degrade coloured aromatic compounds effectively (Vujevic et al., 2010). The main mechanism of Advanced Oxidation Processes, AOPs is the generation of highly reactive hydroxyl radicals, OH· (Gümüş and Akbal, 2011). OH· radicals are electrophiles that react with most electron-rich organic compounds such as dyes to decompose them into less harmful compounds such as carbon dioxide and water (Chan et al., 2011). There are several methods of AOP that are currently in practice to treat dye wastewater such as

Fenton oxidation, ultrasonic cavitation and photochemical oxidation. Fenton oxidation involves the production of reactive OH· under acidic condition through catalytic decomposition of hydrogen peroxide (Güçlü et al., 2013). However, complexity of Fe(III) hydrolysis and its high impact on reaction rates require additional care to obtain well-defined iron salt solutions (Sievers, 2011). On the other hand, ultrasonic cavitation arises from acoustic cavitation, namely the formation, growth and implosive collapse of bubbles in liquids, which generates OH· for chemical reactions (Wu et al., 2013). Ultrasonic cavitation usually incurs higher capital and maintenance cost as compared to ozone or UV treatment due to the energy loss in the ultrasonic system (Chowdhury and Viraraghavan, 2009). Photochemical oxidation was chosen in this study because of its high efficiency in mineralization of organic compounds and feasibility with sunlight (Ong et al., 2012). Titanium (IV) dioxide or TiO_2 was chosen as a photocatalyst for its non-toxicity, high photostability, chemical inertness and resistivity against chemical corrosion (Kavitha and Palanisamy, 2010; Tabaei et al., 2012). In addition, TiO_2 has higher photoreactivity due to its slower electron-hole recombination as compared to zinc oxide, Hombikat, cadmium sulphide, zinc sulphide and iron (III) oxide. Due to relatively low specific surface area of standard TiO_2 powder, TiO_2 nanopowder was used in order to provide more active sites (Low et al., 2012).

The reaction pathway of MB degradation through generation of radicals from photogenerated electron-hole pairs (e_{CB}^- , h_{VB}^+) is shown as follow:

$$TiO_2 + MB \leftrightarrow TiO_2\text{-}MB \quad (1)$$

$$TiO_2\text{-}MB + h\nu \leftrightarrow (e_{CB}^- , h_{VB}^+)\text{-}MB \quad (2)$$

$$h_{VB}^+ + H_2O \rightarrow OH\cdot + H^+ \quad (3)$$

104 $h_{VB}^{+} + OH^{-} \rightarrow OH\cdot$ (4)

105 $e_{CB}^{-} + O_2 \rightarrow O_2^{-}\cdot$ (5)

106 $OH\cdot$ + MB → intermediate products → degradation products (6)

107 $O_2^{-}\cdot$ + MB → intermediate products → degradation products (7)

108 Eq. (1): Adsorption-desorption equilibrium is achieved between TiO_2 catalyst surface and MB
109 during stirring process in the dark.

110 Eq. (2): TiO_2-MB suspension is exposed to sunlight. TiO_2 has band gap energy of 3.2 eV (Zhou
111 et al., 2012). Only light energy with photons greater than the band gap energy is able to excite
112 electrons from the valence band to the conductive band of TiO_2 (Song and Bai, 2010).
113 Therefore, e_{CB}^{-} and h_{VB}^{+} are generated.

114 Eqs. (3)-(4): Photogenerated holes in the valence band react with adsorbed water molecules
115 and hydroxide ions on the catalyst surface to form hydroxyl radical (Wu and Chern, 2006;
116 Gümüş and Akbal, 2011).

117 Eq. (5): The photogenerated electrons in the conduction band are scavenged and react with
118 oxygen molecules that are adsorbed on the catalyst surface to form superoxide radical ions
119 (Wu and Chern, 2006).

120 Eqs. (6)-(7): The generated hydroxyl radicals and superoxide anion radicals from Eqs. (3)-(4)
121 react with MB and degrade it into less harmful products such as carbon dioxide, nitrate,
122 ammonium and sulphate ions (Houas et al., 2001).

123 Although previous studies investigated the degradation of synthetic dye wastewater using
124 photocatalysis, most of the past studies focused on the use of pure or modified catalyst under
125 UV or visible light as a light source (Lee et al., 1999; Houas et al., 2001; Lachheb et al., 2002;

126 Li and Li, 2002; Chen et al., 2003; Lin et al., 2007; Su et al., 2012). In many countries, both
127 energy and waste management systems are under changes (Nouri et al., 2012). Thus, the
128 present study utilized natural sunlight and commercially available catalyst in photocatalytic
129 treatment of MB wastewater. In tropical countries like Malaysia, ample sunlight is available
130 throughout the year, leading to more favourable, sustainable and economical photocatalytic
131 process using sunlight as a light source (Pardeshi and Patil, 2009).

132 Textile industrial wastewater comprises of several chemical and organic compounds, such
133 as salts, detergents, organic acids, dyestuffs, dying aids, and sizing agents (Fu et al., 2011;
134 Lotito et al., 2012). The degradation of those organic substrates leads to the generation of ions,
135 such as chloride and carbonate ions, that may inhibit photocatalysis (Wang et al., 2000; Mota
136 et al., 2008). Past studies reported a decrease in photocatalytic activity of up to 20-30% in the
137 presence of Cl^- and CO_3^{2-} (Lee et al., 1999; Zhou et al., 2010).Therefore, it is crucial to
138 investigate the effect of inhibitors (Cl^- and CO_3^{2-}) on the photocatalytic degradation of MB.

139 On the other hand, the roles of enhancers, namely hydrogen peroxide (H_2O_2) and
140 persulphate ions ($S_2O_8^{2-}$), in photocatalysis of MB were also studied to determine their
141 significance during photodegradation. H_2O_2 was reported as an oxidant that enhanced photo-
142 oxidation treatment in small quantity (Boroski et al., 2008). The use of persulphate ions,
143 $S_2O_8^{2-}$ have attracted increasing attention due to their greater oxidizing potential (1.82-2.02 V)
144 as compared to H_2O_2 (1.76 V) (Chen et al., 2012). For examples, H_2O_2 and $S_2O_8^{2-}$ enabled
145 two-fold increases in decolorization of Maxilon Navy dye and methyl orange, respectively
146 (Ghaly et al., 2007; Anandan, 2008). Thus, the effect of enhancers (H_2O_2 and $S_2O_8^{2-}$) on the
147 photocatalytic degradation of MB was also investigated in this study.

148 To the best of our knowledge, no significant studies were previously conducted on
149 utilizing sunlight and unmodified TiO_2 for photocatalytic treatment of MB under the influence
150 of enhancers or inhibitors which were found in dye industries. Thus, the main goal of the
151 present study was to investigate the recommended conditions and effects of various operating
152 parameters such as (a) initial concentration of MB; (b) initial pH of solution; (c) catalyst
153 dosage; (d) hydrogen peroxide, persulphate ions, chloride ions and carbonate ions on the
154 decolourization efficiency of MB. The kinetic model on decolourization of MB using natural
155 sunlight in Malaysia was also investigated.
156

2 Materials and Methods

2.1 Materials

MB dye with 98.7% purity, (molecular weight of 319.85g/mol and λ_{max} at 664nm) was purchased from Sigma-Aldrich (USA) and it was used without further purification. The molecular structure of MB is illustrated in Fig. 1. TiO_2 nanopowder with 99.7% purity was purchased from Sigma-Aldrich (USA) and used as photocatalyst without further modification. The TiO_2 nanopowder has particle size of < 25 nm and a specific surface area of 200-220 m^2/g. The initial pH value of the MB dye solution was adjusted by using 1 mol/L HCL or 1 mol/L NaOH solution.

2.2 Photoreactor and sunlight illumination

The photoreactor was 17 cm × 11 cm × 5 cm (Length x Width x Depth) in dimension with volume capacity of 650 ml. The photoreactor was set up on a magnetic stirrer at an open space under maximum sunlight exposure. Sunlight intensity was measured using a WalkLAB Digital Lux meter (Trans Instruments (S) Pte. Ltd., Singapore).

2.3 Experimental procedures

MB solution of 500 ml was prepared at desired initial concentration (30-70 ppm), initial pH value (7.5-13.5) and catalyst loading (0.5-2.5 g/L). The concentration range chosen in the present study based on the discharge concentration of a dye plant in Malaysia. The concentration range was chosen in the present study based on approximately the discharge concentration of a dye plant in Malaysia. Furthermore, the presence of a very small amount of dye in water (<1 mg/L for some dyes) is highly visible and enough to present an aesthetic problem (Low et al., 2012). The solution was stirred in the dark for 30 minutes to achieve adsorption-desorption equilibrium. The suspension was then continuously stirred under sunlight from 11 am to 3 pm, during which, the natural sunlight in Malaysia had stable illuminance in the range of 80 to 110 klux. Therefore, all experimental runs were conducted during the aforementioned time frame. The treated MB was sampled every 30 minutes and was centrifuged at 14000 rpm for 15 minutes using Profuge 14k Centrifuge to separate the TiO_2 catalyst. Then, the decolourization efficiency was observed by measuring the absorbance of the supernatant using GENESYS 10UV spectrophotometer (Thermo Fisher Scientific Inc, USA) at a wavelength of 664 nm. The decolourization efficiency was determined by:

$$\text{Decolourization efficiency (\%)} = (C_o - C_{f,t}) / C_o \times 100\% \quad (8)$$

where C_o is the initial dye concentration (mg/l) and $C_{f,t}$ is the final concentration (mg/l) after photodecolourization at time t. Experiments were conducted at surrounding temperature and repeated three times to demonstrate the reproducibility of results. The effects of hydrogen peroxide (510-4080 ppm), persulphate ions (510-4080 ppm), chloride ions (500-2000 ppm) and carbonate ions (500-2000 ppm) were evaluated subsequently using the predetermined

194 recommended conditions of initial concentration of MB, catalyst loading and initial pH. All
195 enhancers and inhibitors were prepared as stock solutions and added into the photocatalytic
196 system following the desired concentration. Control experimental runs were carried out as
197 tabulated in Table 1. Finally, kinetic analysis was performed on all effects.

198 **3 Results and discussion**

199 3.1 Effect of initial concentration

200 Generally, composition of MB in dye wastewater may vary. Hence, it is of interest to study the
201 influence of intial concentration of MB on the decolourization efficiency. Controls A and B
202 (Figs. 2-4) proved that decolourization of MB was not feasible in the absence of natural
203 sunlight and photocatalyst. On the other hand, the use of natural sunlight and photocatalyst
204 resulted in significant MB decolourization efficiency (Figs. 2-8). Fig. 2 shows that when the
205 initial concentration of MB increased from 30 to 70 ppm, the decolourization efficiency of
206 MB decreased. The increase in MB concentration resulted in an increase of MB molecules.
207 Hence, light penetration into the solution was reduced (Akbal, 2005), decreasing the path
208 length of photons entering the solution (Muruganandham et al., 2007). The number of active
209 sites to generate hydroxyl radicals decreased due to the fewer photons reaching the catalyst
210 surface. Therefore, photocatalytic activity decreased with increasing initial concentration of
211 MB.

212 Fig. 2 shows that there was still a very minimal decolourization of 5.5% in the dark for
213 control A. This was due to the adsorption of some MB molecules on TiO_2 catalyst surface
214 (Kansal et al., 2007). Therefore, minimal decolourization was observed albeit in the absence
215 of sunlight. Decolourization of 13.0% was also observed in the absence of TiO_2 for control B
216 (Fig. 2). This was due to the excitation of MB molecules when they were irradiated under

sunlight which led to direct degradation of MB (Hashim et al., 2001). However, the decolourization in the absence of catalyst (control B) was ineffective as compared to the presence of catalyst. Generally, an increase in initial dye concentration reduces the decolourization efficiency (Neppolian et al., 2002). However, the present study showed no significant difference in maximum decolourization of MB between the initial concentrations of MB from 30 to 60 ppm after 4 hours of photodecolourization (Fig. 2). In addition, 60 ppm was the highest initial concentration to achieve at least 80% of maximum decolourization. Therefore, an initial concentration of 60 ppm would be used for the subsequent investigations.

Literature reviews suggested that heterogeneous photocatalysis follows the Langmuir-Hinshelwood, L-H kinetic expression as shown in Eq. (8). It is deemed the most appropriate model to describe a plateau-type kinetic profile (Figs. 2-8) in which the rate of decolourization increases with photodecolourization time until the rate becomes zero (Yang et al., 2005; Pouretedal and Kadkhodaie, 2010).

$$r = -\frac{dC}{dt} = \frac{kK_{dye}C}{1 + K_{dye}C_{initial}} \tag{9}$$

Eq. (9): $C_{initial}$ is the initial concentration of MB (ppm or mg/L). K_{dye} is the L-H adsorption equilibrium constant, (L/mg) and it represents the catalyst adsorption capacity. k is the rate constant of the surface reaction (mg/L.min) and it is the proportionality constant for the intrinsic reactivity of photo-activated surface with C.

At low initial concentration of MB (< 300 ppm), Eq. (9) can be simplified into a pseudo-first-order equation as shown in Eq. (10) (Nezamzadeh-Ejhieh and Hushmandrad, 2010).

$$r = -\frac{dC}{dt} = k_{app}C \tag{10}$$

238 Eq. (9): k_{app} (min^{-1}) is the pseudo-first-order rate constant and it serves as a comparison and
239 description for the photocatalytic reaction rate in the reactor system (Low et al., 2012).

240 Further integration and rearranging of Eqs. (10), (11) and (12) are obtained (Low et al.,
241 2012). Straight line plots of ln C against time yielded k_{app} values for different effects (Table 2-
242 3). k_{app} values were used for the kinetic study of this research.

243 $$C = C_0 e^{-k_{app} t} \quad (11)$$

244 $$\ln C = -k_{app} t + \ln C_0 \quad (12)$$

245

246 k_{app} for 70 ppm was 54% lower than 30 ppm (Table 2). Reduction in k_{app} values at higher
247 initial concentration of MB (Table 2) further proved that the increase in initial concentration of
248 dye led to a decrease in photocatalytic activity.

249

250 3.2 Effect of catalyst loading

251 In order to reduce the economical cost of using large quantity of catalyst, it is of great desire to
252 achieve high decolourization efficiency with minimal usage of catalyst loading during
253 wastewater treatment process. Therefore, the recommended catalyst loading for effective MB
254 decolourization was investigated in the present study. Fig. 3 and Table 2 show that at lower
255 TiO_2 loading, lower percentage of decolourization and k_{app} values were observed due to the
256 lacking of catalyst (such as 0.5 g/L of catalyst loading) to fully utilize the transmitted light to
257 form active sites (Kavitha and Palanisamy, 2010). As the catalyst dosage gradually increased
258 from 0.5 to 1.5 g/L, more catalyst was present in the solution to be activated by photons,
259 hence, more active sites were generated, which in return generated more hydroxyl radicals

(Lee et al., 1999). Thus, the number of MB molecules adsorbed on active sites and decolourized by hydroxyl radicals increased. Therefore, photocatalytic activity accelerated when catalyst loading increased gradually. An increase of k_{app} values from 0.5 to 1.5 g/L of catalyst dosage is shown in Table 2.

However, Fig. 3 also shows that the decolourization of MB decreased when the catalyst loading was further increased above 1.5 g/L (2.0 to 2.5 g/L). This phenomenon was attributed to an excessive amount of TiO_2 present in the solution that contributed towards higher suspension turbidity in the solution (Lee et al., 1999). Thus, light scattering increased due to the presence of excessive catalyst which reduced light penetration (Franco et al., 2009; Herney-Ramirez et al., 2010). Fewer photons reached and activated the catalyst surface, leading to the reductions of active sites and fewer generations of hydroxyl radicals (Franco et al., 2009). In short, further addition of catalyst dosage beyond a specific limit did not enhance the photocatalytic activity but deteriorated it. Similar phenomenon was observed by Xiao et al. (2008), who found that an increase of catalyst loading from 0.5 to 1.0 g/L enhanced the decolourization of MB but a decline in efficiency was observed when higher dosage of catalyst was used (> 1.0 g/L). Based on Fig. 3 and Table 2, catalyst loading of 1.5 g/L achieved the highest decolourization efficiency and pseudo-first-order rate constant. However, the difference in maximum decolourization efficiency between 1.0 and 1.5 g/L was insignificant whereby the former and later achieved 85.8 and 91.7%, respectively. Apart from that, smaller catalyst dosage is less economical costing for industrial practices as compared to the use of higher catalyst dosage with similar decolourization efficiency outcome. Therefore, catalyst loading of 1.0 g/L was the chosen catalyst dosage for the subsequent investigations.

3.3 Effect of initial pH

In general, dye wastewater discharged from industries has a wide range of pH values. Since the generation of hydroxyl radicals is affected by pH conditions, the variation of pH should be taken into account in the treatment of dye wastewater. Study on the influence of initial pH showed that the decolourization of MB and pseudo-first-order rate constants increased with increasing pH from 7.5 to 13.5 as shown in Fig. 4 and Table 2. MB dissolved as a cationic dye in aqueous solution. The surface charge of TiO_2 catalyst became more negative as the pH of the solution increased. Hence, a stronger adsorption was formed between the positively charged MB cations and negatively charged TiO_2 surface due to electrostatic interaction (Senthilkumaar et al., 2006). Therefore, a higher rate of decolourization was achieved at higher pH values.

An increase of k_{app} values could be observed when the treatment process was conducted in more alkaline condition (Table 2). Based on Fig. 4, the lowest initial pH to achieve at least 80% maximum decolourization efficiency was pH 10.5. Although initial pH 12 and 13.5 exhibited higher maximum decolourization efficiency (Fig. 4) and at a faster rate (Table 2) as compared to 10.5, the selection of high pH is not favorable in wastewater treatment. The treated wastewater with higher initial pH value may impose a detrimental effect on any downstream biological treatment process, especially to methanogenic bacteria during anaerobic digestion (Appels et al., 2008). In addition, the increasing use of alkaline chemicals is not environmentally sustainable and economically sound. Therefore, initial pH 10.5 was selected for the subsequent investigations instead of initial pH 12 or 13.5.

307

308 3.4 Influence of enhancers

309 The use of enhancers (H_2O_2 and $S_2O_8^{2-}$) in the absence of sunlight and TiO_2 as a photocatalyst
310 (controls C-F) resulted in insignificant decolourization efficiency of MB. On the other hand,
311 H_2O_2 and $S_2O_8^{2-}$ experimental runs that were conducted under sunlight together with TiO_2
312 resulted in higher decolourization efficiency (Figs. 5-6). The results showed that higher
313 decolourization efficiency using H_2O_2 and $S_2O_8^{2-}$ could only be attained under sunlight and in
314 the presence of TiO_2. Subsequent investigations on the use of H_2O_2 and $S_2O_8^{2-}$ were performed
315 under sunlight and in the presence of TiO_2.

316

317 3.4.1 Hydrogen peroxide, H_2O_2

318 Rate of decolourization of dye wastewater can be significantly improved due to the presence
319 or addition of certain substances such as hydrogen peroxide (H_2O_2) (Giri et al., 2011). In order
320 to treat large capacity of dye wastewater, certain treatment plants choose to add photo-
321 assisting chemicals to degrade non-biodegradable pollutants more effectively (Lee et al.,
322 2011). Hence, this study investigated the influence of H_2O_2 on the decolourization of MB.
323 Results from Fig. 5 shows that the control O (without additive) achieved lower decolourization
324 efficiency as compared to experiments with H_2O_2 addition. According to Table 3, there was a
325 significant increase of 513% in k_{app} values between the absence of H_2O_2 and 4080 ppm of
326 H_2O_2. As the concentration of H_2O_2 added into the solution increased, the decolourization
327 efficiency (Fig. 5) and pseudo-first-order rate constants (Table 2) increased. H_2O_2 has electron
328 scavenging properties. Hence, H_2O_2 reacted with electrons from the conduction band of TiO_2
329 to form hydroxyl radicals (Mohapatra and Parida., 2006). An increase in concentration of

H_2O_2 led to an increase number of hydroxyl radicals generation, hence, more MB molecules would be degraded by hydroxyl radicals. Therefore, decolourization efficiency increased with an increase of H_2O_2. Although in the absence of catalyst, a significant decolourization of 35.5% was observed for control D (Fig. 5). This phenomenon was attributed to the direct breakdown of H_2O_2 under sunlight to form hydroxyl radicals (Kavitha and Palanisamy, 2010).

For control C, slight decolourization of 14.3% was observed. This was due to adsorption of MB molecules on catalyst surface. Thus, slight decolourization occurred although in the absence of sunlight. By comparing the decolourization results obtained for control C against 510-4080 ppm of H_2O_2 under sunlight (Fig. 5), the influence of H_2O_2 was much significant under sunlight because sunlight was able to accelerate the generation of active sites and direct breakdown of H_2O_2 (Kavitha and Palanisamy, 2010). Hydroxyl radical was formed based on the three reaction pathways as shown below (Kavitha and Palanisamy, 2010):

$$e_{CB}^- + H_2O_2 \rightarrow OH\cdot + OH^- \quad (13)$$

$$H_2O_2 + O_2^{-}\cdot \rightarrow OH\cdot + H^+ + O_2 \quad (14)$$

$$H_2O_2 + h\nu \rightarrow 2\ OH\cdot \quad (15)$$

Eq. (13): When active sites are formed from TiO_2 under sunlight, H_2O_2 traps photogenerated electrons from the conduction band of TiO_2 to generate hydroxyl radicals, inhibiting electron-hole recombination.

Eq. (14): H_2O_2 reacts with superoxide anion generated from Eq. (5) to form hydroxyl radicals.

Eq. (15): H_2O_2 also converts directly into hydroxyl radicals under sunlight.

3.4.2 Persulphate ions, $S_2O_8^{2-}$

352 Fig. 6 shows that the decolourization efficiency obtained by 0 ppm $S_2O_8^{2-}$ was lower as
353 compared to the experiments with $S_2O_8^{2-}$ addition whereas there was an 743% increase in k_{app}
354 values between 0 ppm and 4080 ppm of $S_2O_8^{2-}$ (Table 3). The present result verified that the
355 addition of $S_2O_8^{2-}$ could significantly improve the decolourization efficieny of MB. $S_2O_8^{2-}$
356 showed a silmiar trend as H_2O_2, in which a gradual increase in $S_2O_8^{2-}$ resulted in significant
357 increase of MB decolourization because $S_2O_8^{2-}$ has electron scavenging properties (Das et al.,
358 2007). Hence, $S_2O_8^{2-}$ reacted with electrons from the conduction band of TiO_2 to form sulphate
359 radical anions. Sulphate radical anions would then react with water molecules to form
360 hydroxyl radicals. In short, an increase in concentration of $S_2O_8^{2-}$ led to an increase of both
361 sulphate radical anions and hydroxyl radicals. Therefore, decolourization efficiency increased
362 with increasing $S_2O_8^{2-}$.

363 Secondly, the generation of sulphate radical anions from $S_2O_8^{2-}$ also prevented electron-
364 hole recombination of TiO_2 (Kavitha and Palanisamy, 2010). When the concentration of $S_2O_8^{2-}$
365 increased, electrons in the conduction band of TiO_2 were continuously consumed by more
366 sulphate radical anions, resulting more valence band electrons would be promoted into the
367 conduction and leaving behind more photogenerated holes in the valence band. According to
368 Eqs. (3) and (4), more hydroxyl radicals could be generated in the presence of more
369 photogenerated holes. Therefore, decolourization efficiency was improved with an addition of
370 $S_2O_8^{2-}$. Thirdly, sulphate radical anions could react and degrade MB. Sulphate radical anions
371 also had a unique nature of attacking MB molecules in various positions which resulted in
372 fragmentation of MB molecules to occur rapidly (Neppolian et al., 2002). Therefore,
373 decolourization efficiency of MB increased when concentration of $S_2O_8^{2-}$ increased.

374 Control E and F (Fig. 6) had a higher maximum decolourization efficiecny as compared to
375 control C and D of H_2O_2 (Fig. 5). This phenomenon was due to strong oxidizing properties of
376 $S_2O_8^{2-}$ (Das et al., 2007). Sulphate radical anions formed from $S_2O_8^{2-}$ could react and degrade
377 MB molecules in the absence or presence of sunlight (Das et al., 2007). Therefore, $S_2O_8^{2-}$
378 addition in the dark was able to decolourize MB effectively. The following reaction pathways
379 summarize the photocatalytic activity of MB with an addition of $S_2O_8^{2-}$.

380 $$S_2O_8^{2-} + e_{CB}^- \rightarrow SO_4^-\cdot + SO_4^{2-} \quad (16)$$

381 $$SO_4^- + H_2O \rightarrow OH\cdot + SO_4^{2-} + H^+ \quad (17)$$

382 $$SO_4^-\cdot + e_{CB}^- \rightarrow SO_4^{2-} \quad (18)$$

383 $$SO_4^-\cdot + MB \rightarrow SO_4^{2-} + MB^+\cdot \text{ (intermediates)} \quad (19)$$

384 $$SO_4^-\cdot + MB^+\cdot \text{ (intermediates)} \rightarrow SO_4^{2-} + CO_2 + HNO_3 + \text{other inorganic} \quad (20)$$

385 Eq. (16): $S_2O_8^{2-}$ possesses electron scavenging properties and reacts with electrons from the
386 conduction band of TiO_2 to form sulphate radical anions (Kavitha and Palanisamy, 2010).
387 Eq. (17): Sulphate radical anions react with water molecules to generate hydroxyl radicals
388 (Das et al., 2007).
389 Eq. (18): Sulphate radical anions trap photogenerated electrons from the conduction band of
390 TiO_2 to prevent electron-hole recombination (Neppolian et al., 2002).
391 Eqs. (19)-(20): Sulphate radical anions are powerful oxidants that react and degrade MB
392 molecules (Das et al., 2007).
393
394
395

396 3.5 Influence of inhibitors

397 The use of inhibitors (Cl^- and CO_3^{2-}) in the absence of sunlight and TiO_2 as photocatalyst
398 (controls G-J) showed no improvement in decolourization efficiency of MB. Therefore,
399 subsequent investigations relating to the use of Cl^- and CO_3^{2-} were carried out under sunlight
400 and presence of TiO_2.

401

402 3.5.1 Chloride ions, Cl^-

403 Sodium chloride is found in dye wastewater as a result of sectional waste from textile mills
404 (Neppolian et al., 2002). Therefore, it is important to determine the treatment efficiency of
405 photocatalysis under the influence of Cl^-. Results obtained (Fig. 7 and Table 2) in this study
406 showed that the rate of decolourization decreased with increasing amount of Cl^-. Furthermore,
407 a decrease in k_{app} values from 10.8×10^{-3} (0 ppm of Cl^-) to 7.8×10^{-3} (2000 ppm of Cl^-)
408 indicated a decline in photocatalytic activity. A consumption of photogenerated holes by Cl^-
409 inhibited the generation of hydroxyl radicals (Eqs. 3 and 4), which in turn resulted in the
410 reduction of photocatalytic activity (Neppolian et al., 2002). Therefore, Cl^- exhibited strong
411 inhibiting effects for MB degradation, whereby an increase of Cl^- led to a decrease in
412 decolourization efficiency of MB.

413 Slight higher decolourization efficiency was observed for control G as compared to
414 control H (Fig. 7). This phenomenon was attributed to some of the MB molecules adsorbed on
415 the catalyst surface for control G. Therefore, percentage of decolourization for 2000 ppm Cl^-
416 in the dark was slightly higher than 2000 ppm under sunlight without catalyst. The inhibition

417 of OH· generation due to the consumption of photogenerated holes by Cl^- could be explained
418 by using two reaction pathways as shown below (Neppolian et al., 2002; Gaca et al., 2005):

419 $Cl^- + h_{VB}^+ \rightarrow Cl\cdot$ (21)

420 $Cl\cdot + Cl^- \rightarrow Cl_2^-\cdot$ (22)

421 Eq. (21): Cl^- reacts with photogenerated holes from valence band of TiO_2 to form chlorine
422 radicals.

423 Eq. (22): Chlorine radicals then react with Cl^- and convert into chloride radical anion.

424

425 3.5.2 Carbonate ions, CO_3^{2-}

426 Sodium carbonate is commonly used in textile processing operations to adjust the pH of the
427 dying bath (Neppolian et al., 2002). Hence, dye wastewater from textile industries may
428 contain traces of sodium carbonate. The present study also investigated the influence of CO_3^{2-}
429 on the decolourization efficiency of MB. Fig. 8 and Table 2 show that the percentage of
430 decolourization and k_{app} values decreased when the concentration of CO_3^{2-} increased. A
431 decrease in k_{app} values from 10.8 (0 ppm of CO_3^{2-}) to 7.3×10^{-3} min^{-1} (2000 ppm of CO_3^{2-})
432 further proved that the photocatalytic activity of MB declined with an increase of CO_3^{2-}. The
433 decrease in decolourization efficiency of MB was attributed to the hydroxyl radicals
434 scavenging properties of CO_3^{2-} (Lee et al., 1999). CO_3^{2-} reacted with hydroxyl radicals, hence,
435 reducing the number of hydroxyl radicals available. The decrease in hydroxyl radicals, which
436 served as a primary source for photodegradation of MB, reduced the decolourization
437 efficiency. Therefore, in photocatalytic process, CO_3^{2-} inhibited the degradation of MB. The
438 role of CO_3^{2-} could be explained by the following reaction pathway (Neppolian et al., 2002):

439 $CO_3^{2-} + OH\cdot \rightarrow CO_3^{-} + OH^{-}$ (23)

440 Eq. (23): CO_3^{2-} is consumed by reacting with hydroxyl radicals to generate carbonate radical
441 anion as oxidation transients.

442

443 3.6 Comparison of k_{app} values under the influence of enhancer and inhibitor

444 By comparing k_{app} values obtained for the experimental run without additives (Table 3), the
445 presence of H_2O_2 and $S_2O_8^{2-}$ increased the rate of photodecolourization by 38-513% and 36-
446 743%, respectively. On the other hand, an addition of Cl^- and CO_3^{2-} reduced the rate of
447 photodecolourization of MB by 15-28% and 13-32%, respectively. k_{app} values for both 2040
448 and 4080 ppm of $S_2O_8^{2-}$ were significantly higher as compared to the similar concentration of
449 H_2O_2 (Table 3). Thus, the results from the present study agreed with Poulios and Aetopoulou
450 (1999), that $S_2O_8^{2-}$ was a more powerful oxidizing agent in decolourizing MB as compared to
451 H_2O_2. However, the inhibitor strengths between Cl^- and CO_3^{2-} remained inconclusive due to
452 the similar k_{app} values obtained for both anions.

453 The value of k_{app} obtained from this study for different initial concentration of MB was
454 summarized and compared with the previous studies (Table 4). In general, higher values of
455 k_{app} were obtained in most of the past studies (Table 4). However, their results were mainly
456 attributed to the use of UV light source, lower concentration of MB and/or higher
457 concentration of TiO_2. The present study was performed comparatively good with k_{app} of 10.8
458 $\times 10^{-3}$ min^{-1} at 60 ppm MB and 1 g/L TiO_2 under sunlight up to 240 min. Under same
459 condition, the k_{app} was increased by 743% to 91.0 $\times 10^{-3}$ min^{-1} with an addition of 4080 ppm
460 $S_2O_8^{2-}$. Thus, this study indicated that higher concentration of MB could be treated under

461 tropical sunlight through photocatalytic process if certain amount of persulphate ions was
462 added into the treatment system. However, further investigations are needed to confirm the
463 effective use of persulphate ions under sunlight during the photocatalytic treatment of
464 wastewater, which consists of multiple dyes.
465
466 **4 Conclusions**
467 By studying the effects of initial concentration, initial pH and catalyst loading, it was found
468 that 85.2% of 60 ppm MB was successfully decolourized under 1.0 g/L of TiO_2 dosage and
469 initial pH 10.5. An increase of initial concentration but a decrease of pH would result in a
470 reduction of photocatalytic treatment of MB. The gradual increase of catalyst loading resulted
471 in the gradual increase of decolourization efficiency but further addition of catalyst after the
472 recommended catalyst dosage did not increase photocatalytic activity. An addition of strong
473 oxidizing agents such as H_2O_2 and $S_2O_8^{2-}$ further enhanced the photocatalytic activity of MB
474 up to 96.6% and 99.3%, respectively. In addition, persulphate ions concluded to be a stronger
475 oxidizing agent as compared to hydrogen peroxide. On the other hand, the presence of Cl^- and
476 CO_3^{2-} inhibited photocatalytic activity up to 74.7% and 70.2%, respectively.
477 In conclusions, this study proved that it is possible to achieve high decolourization
478 efficiency of dye using photocatalytic treatment under natural sunlight in a tropical country
479 like Malaysia, where an abundance of sunlight is made available throughout the year. It is an
480 economical and environmentally sustainable method to utilize sunlight as a natural source of
481 energy to treat dye wastewater through photocatalytic process.
482
483

Acknowledgements

The authors would like to thank Monash University, Sunway campus for providing W. Subramonian with a PhD scholarship.

488 **References**

489 Advanced Dyestuff and Chemicals Pvt. Ltd., 2011. Product List for Textile Applications.
490 http://www.textiledyes.net/textile-dyes.html. Accessed: 1 May 2011.

491 Akbal, F. (2005). Photocatalytic degradation of organic dyes in the presence of titanium oxide
492 under UV and solar light: effect of operational parameters. *Environmental Progress,*
493 *24*, 317-322.

494 Álvarez, M. S., Moscoso, F., Rodríguez, A., Sanromán, M. A., & Deive, F. J. (2013). Novel
495 physic-biological treatment for the remediation of textile dyes-containing industrial
496 effluents. *Bioresource Technology, 146*, 689-695.

497 Anandan, S. (2008). Photocatalytic effects of titania supported nanoporous MCM-41 on
498 degradation of Methyl Orange in the presence of electron acceptors. *Dyes and*
499 *Pigments, 76*, 535-541.

500 Appels, L., Baeyens, J., Degrève, J., & Dewil, R. (2008). Principles and potential of the
501 anaerobic digestion of waste-activated sludge. *Progress in Energy and Combustion*
502 *Science, 34*, 755-781.

503 Boroski, M., Rodrigues, A. C., Garcia, J. C., Gerola, A. P., Nozaki, J., & Hioka, N. (2008).
504 The effect of operational parameters on electrocoagiulation-flotation process followed
505 by photocatalysts applied to the decontamination of water effluents from cellulose and
506 paper factories. *Journal of Hazardous Materials, 160*, 135-141.

507 Chan, S. H. S., Wu, T. Y., Juan, J. C., & Teh, C. Y. (2011). Recent developments of metal
508 oxide semiconductors as photocatalysts in advanced oxidation processes (AOPs) for

509 treatment of dye wastewater. *Journal of Chemical Technology and Biotechnology, 86*,
510 1130-1158.

511 Chen, F., Zhao, J., & Hidaka, H. (2003). Adsorption factor of dye constituent aromatics on the
512 surface of TiO_2 in the presence of phosphate ions. *Research on Chemical*
513 *Intermediates, 29*, 733-748.

514 Chen, X., Wang, W., Xiao, H., Hong, C., Zhu, F., Yao, Y., & Xue, Z. (2012). Accelerated
515 TiO_2 photocatalytic degradation of Acid Orange 7 under visible light mediated by
516 peroxymonosulphate. *Chemical Engineering Journal, 193-194*, 290-295.

517 Chiu, W. S., Khiew, P. S., Cloke, M., Isa, D., Tan, T. K., Radiman, S., Abd-Shukor, R.,
518 Hamid, A. M. A., Huang, N. M., Lim, H. N., & Chia, C. H. (2010). Photocatalytic
519 study of two-dimensional ZnO nanopellets in the decomposition of Methylene
520 Blue. *Chemical Engineering Journal, 158***,** 345-352.

521 Chowdhury, P., & Viraraghavan, T. (2009). Sonochemical degradation of chlorinated organic
522 compounds, Phenolic Compounds and Organic Dyes –A Review. *Science of the Total*
523 *Environment, 407*, 2474-2492.

524 Das, D. P., Baliarsingh, N., & Parida, K. M. (2007). Photocatalytic decolorisation of
525 Methylene Blue (MB) over titania pillared zirconium phosphate (ZrP) and titanium
526 phosphate (TiP) under solar radiation. *Journal of Molecular Catalysis A: Chemical,*
527 *261*, 241-261.

528 Forgacs, E., Cserháti, T., & Oros, G. (2004). Removal of synthetic dyes from wastewaters: a
529 review. *Environmental International, 30*, 953-971.

530 Franco, A., Neves, M. C., Carrott, M. M. L., Mendonca, M. H., Pereira, M. I., & Monteiro, O.
531 C. (2009). Photocatalytic decolorization of Methylene Blue in the presence of
532 TiO_2/ZnS nanocomposites. *Journal of Hazardous Materials, 161*, 545-550.
533 Fu, Z., Zhang, Y., & Wang, X. (2011). Textile wastewater treatment using anoxic filter bed
534 and biological wriggle bed-ozone biological aerated filter. *Bioresource Technology,*
535 *102*, 3748-3753.
536 Gaca, J., Kowalska, M., & Mróz, M. (2005). The effect of chloride ions on
537 alkylbenzenesulfonate degradation in the Fenton reagent. *Polish Journal of*
538 *Environmental Studies, 14*, 23-27.
539 Ghaly, M. Y., Farah, J. Y., & Fathy, A. M. (2007). Enhancement of decolorization rate and
540 COD removal from dyes containing wastewater by the addition of hydrogen peroxide
541 under solar photocatalytic oxidation. *Desalination, 217*, 74-84.

542 Ghaly, M. Y., Jamil, T. S., El-Seesy, I. E., Souaya. E. R., & Nasr, R.A. (2011). Treatment of
543 highly polluted paper mill wastewater by solar photocatalytic oxidation with
544 synthesized nano TiO_2. *Chemical Engineering Journal, 168*, 446-454.

545 Giri, R. R., Ozaki, H., Takayanagi, Y., Taniguchi, S., & Takanami, R. (2011). Efficacy of
546 ultraviolet radiation and hydrogen peroxide oxidation to eliminate large number of
547 pharmaceutical compounds in mixed solution. *International Journal of Environmental*
548 *Science and Technology, 8*, 19-30.

549 Güçlü, D., Şirin, N., Şahinkaya, S., & Sevimli, M. F. (2013). Advanced treatment of coking
550 wastewater by conventional and modified Fenton processes. *Environmental Progress*
551 *and Sustainable Energy, 32*, 176-180.
552 Gümüş, D., & Akbal, F. (2011). Photocatalytic degradation of textile dye and wastewater.
553 *Water, Air, & Soil Pollution, 216*, 117-124.
554 Hashim, H. A. A., Mohamed, A. R., & Lee, K. T. (2001). Solar photocatalytic degradation of
555 Tartrazine using titanium oxide. *Jurnal Teknologi, 35*, 31-40.
556 Herney-Ramirez, J., Vicente, M. A., & Madeira, L. M. (2010). Heterogeneous photo-Fenton
557 oxidation with pillard clay-based catalysts for wastewater treatment: a review. *Applied*
558 *Catalysis B: Environmental, 98*, 10-26.
559 Houas, A., Lachheb, H., Ksibi, M., Elaloui, E., Guillard, C., & Hermann, J. M. (2001).
560 Photocatalytic degradation pathway of Methylene Blue in water. *Applied Catalysis B:*
561 *Environmental, 31*, 145-157.
562 Kansal, S. K., Singh, M., & Sud, D. (2007). Studies on photodegradation of two commercial
563 dyes in aqueous phase using different photocatalysts. *Journal of Hazardous Materials,*
564 *141*, 581-590.
565 Kavitha, S. K., & Palanisamy, P. N. (2010). Solar photocatalytic degradation of Vat Yellow 4
566 dye in aqueous suspension of TiO_2 - optimization of operational parameters.
567 *International Journal of Bioflux Society, 2*, 189-202.
568 Kitture, R., Koppikar, S. J., Kaul-Ghanekar, R., & Kale, S. N. (2010). Catalyst efficiency,
569 photostability and reusability study of ZnO nanoparticles in visible light for dye
570 degradation. *Journal of Physics and Chemistry of Solids, 72*, 60-66.

571 Kumar, J., & Bansal, A. (2012). Photodegradation of Amaranth in aqueous solution catalyzed
572 by immobilized nanoparticles of titanium oxide. *International Journal of*
573 *Environmental Science and Technology, 9*, 479-484.

574 Kumar, J., & Bansal, A. (2013). A comparative study of immobilization techniques for
575 photocatalytic degradation of Rhodamine B using nanoparticles of titanium dioxide.
576 *Water, Air, & Soil Pollution, 224*, 1-11.

577 Lachheb, H., Puzenat, E., Houas, A., Elalaoui, E., Guilard, C., Hermann, J. M., & Mohamed,
578 K. (2002). Photocatalytic degradation of various types of dyes (Alizarin S,Crocein
579 Orange G, Methyl Red, Congo Red, Methylene Blue) in water by UV-irradiated
580 titania. *Applied Catalysis B: Environmental, 39*, 75-90.

581 Lee, B. N., Liaw, W. D., & Lou, J. C. (1999). Photocatalytic decolorization of Methylene Blue
582 in aqueous TiO_2 suspension. *Environmental Engineering Science, 16*, 165-175.

583 Lee, E., Lee, H., Kim, Y. K., Sohn, K., & Lee, K. (2011). Hydrogen peroxide interference in
584 chemical oxygen demand during ozone based advanced oxidation of anaerobiacally
585 digested livestock wastewater. *International Journal of Environmental Science and*
586 *Technology, 8*, 381-388.

587 Li, F. B., & Li, X. Z. (2002). The enhancement of photodegradation efficiency using Pt-TiO_2
588 catalyst. *Chemosphere, 48*, 1103-1111.

589 Lin, X., Huang, F., Wang, W., & Shi, J. (2007). Photocatalytic activity of $Bi_{24}Ga_2O_{39}$ for
590 degrading Methylene Blue. *Scripta Materialia, 56*, 189-192.

591 Lodha, S., Jain, A., & Punjabi, P. B. (2010). A comparative study of photocatalytic
592 degradation of Methylene Blue in presence of some transition metal complexes and
593 hydrogen peroxide. *Malaysian Journal of Chemistry, 120*, 19-26.
594 Lotito, A. M., Fratino, U., Bergna, G., & Iaconi, C. D. (2012). Integrated biological and ozone
595 treatment of printing textile wastewater. *Chemical Engineering Journal, 195-196*, 261-
596 269.

597 Low, F. C. F., Wu, T. Y., Teh, C. Y., Juan, J. C., & Balasubramaniam, N. (2012).
598 Investigation into photocatalytic decolorisation of CI Reactive Black 5 using titanium
599 dioxide nanopowder. *Coloration Technology, 128*, 44-50.
600 Mohapatra, P., & Parida, K. M. (2006). Photocatalytic activity of sulfate modified titania 3:
601 decolorization of Methylene Blue in aqueous solution. *Journal of Molecular Catalysis*
602 *A: Chemical, 258*, 118-123.
603 Mota, A. L. N., Albuquerque, L. F., Beltrame, L. T. C., Chiavone-Filho, O., Machulek, Jr. A,
604 & Nascimento, C. A. O. (2008). Advanced oxidation process and their application in
605 the petroleum industry: a review. *Brazilian Journal of Petroleum and Gas, 2*, 122-142.
606 Muruganandham, M., Sobana, N., & Swaminathan, M. (2007). Solar assisted photocatalytic
607 and photochemical degradation of Reactive Black 5. *Journal of Hazardous Materials*
608 *B, 137*, 1371-1376.

609 National Toxicology Program, 2013. Executive summary of safety and toxicity information:
610 Methylene Blue. http://ntp.niehs.nih.gov/?objectid=03DB4384-0364-AB0B-
611 5C71EF4A37D6888A#NOM. Accessed 16 October 2013.
612 Neppolian, B., Choi, H. C., Sakthivel, S., Arabindoo, B., & Murugesan, V. (2002). Solar light
613 induced and TiO_2 assisted degradation of textile dye Reactive Blue 4. *Chemosphere,*
614 *46*, 1173-1181.
615 Nezamzadeh-Ejhieh, A., & Hushmandrad, S. (2010). Solar photodecolorization of Methylene
616 Blue by CuO/X zeolite as a heterogeneous catalyst. *Applied Catalysis, 338*, 149-159.
617 Nouri, J., Nouri, N., & Moeeni, M. (2012). Development of industrial waste disposal scenarios
618 using life-cycle assessment approach. *International Journal of Environmental Science*
619 *and Technology, 9*, 417-424.
620 Ong, S.-A., Min, O.-M., Ho, L.-N., & Wong, Y.-S. (2012). Comparative study on
621 photocatalytic degradation of mono azo dye acid orange 7 and methyl orange under
622 solar light irradiation. *Water, Air, & Soil Pollution, 223*, 5483-5493.
623 Pang, Y. L., & Abdullah, A. Z. (2013). Current status of textile industry wastewater
624 management and research progress in Malaysia: A review. *Clean – Soil, Air, Water,*
625 *41*, 751-764.
626 Pardeshi, S. K., & Patil, A. B. (2009). Solar photocatalytic degradation of resorcinol a model
627 endocrine disrupter in water using zinc oxide. *Journal of Hazardous Materials, 163*,
628 403-409.
629 Poulios, I., & Aetopoulou, I. (1999). Photocatalytic degradation of the textile dye Reactive
630 Orange 16 in the presence of TiO_2 suspensions. *Environmental Technology, 20*, 479-
631 487.

632 Pouretedal, H. R., & Kadkhodaie, A. (2010). Synthetic CeO_2 nanoparticle catalysis of
633 methylene blue photodegradation: kinetics and mechanism. *Chinese Journal of*
634 *Catalysis, 31*, 1328-1334.
635 Saheed, H. (2012). Prospects for the textile and clothing industry in Malaysia. *Textile Outlook*
636 *International, 158*, 64-101.
637 Saif Ur Rehman, M., & Han, J. I. (2013). Biosorption of methylene blue from aqueous
638 solutions by *Typha angustata* phytomass. *International Journal of Environmental*
639 *Science and Technology, 10*, 865-870.
640 Senthilkumaar, S., Porkodi, K., Gomathi, R., Maheswari, A. G., & Manomani, N. (2006). Sol
641 gel derived silver doped nanocrystalline titania catalysed photodegradation of
642 Methylene Blue from aqueous solution. *Dyes and Pigments, 69*, 22-30.
643 Sievers, M. (2011). Advanced oxidation processes. *Treatise on Water Science, 4*, 377-408.
644 Song, Y., & Bai, B. (2010). TiO_2-assisted photodegradation of Direct Blue 78 in aqueous
645 solution in sunlight. *Water, Air, & Soil Pollution, 213*, 311-317.
646 Su, T.-L., Kuo, Y.-L., Wu, T.-J., & Kung, F.-C. (2012). Experimental analysis and
647 optimization of the synthesizing property of nitrogen-modified TiO_2 visible-light
648 photocatalysts. *Journal of Chemical Technology and Biotechnology, 87*, 160-164.
649 Sun, D., Zhang, X., Wu, Y., & Liu, T. (2013). Kinetic mechanism of competitive adsorption
650 of disperse dye and anionic dye on fly ash. *International Journal of Environmental*
651 *Science and Technology, 10*, 799-808.

652 Tabaei, H. S. M., Kazemeini, M., & Fattahi, M. (2012). Preparation and characterization of
653 visible light sensitive nano titanium dioxide photocatalyst. *Scientia Iranica C, 19*,
654 1626-1631.

655 Vujevic, D., Papic, S., Koprivanac, N., & Bozic, A. (2010). A decolorization and
656 mineralization of reactive dye by UV/Fenton process. *Separation Science and*
657 *Technology, 45*, 637–1643.

658 Wang, K. H., Hsieh, Y. H., Wu, C. H., & Cheng, C. Y. (2000). The pH and anion effects on
659 the heterogeneous photocatalytic degradation of o-methylebenzoic acid in TiO_2
660 aqueous suspension. *Chemosphere, 40*, 389-394.

661 Wang, S., Li, D., Sun, C., Yang, S., Guan, Y., & He, H. (2014). Highly efficient photocatalytic
662 treatment of dye wastewater via visible-light-driven AgBr-Ag_3PO_4 / MWCNTs.
663 *Journal of Molecular Catalysis A: Chemical, 383-384*, 128-136.

664 Wu, C. H., & Chern, J. M. (2006). Kinetics of photocatalytic decomposition of Methylene
665 Blue. *Industrial and Engineering Chemistry Research, 45*, 6450-6457.

666 Wu, T. Y., Guo, N., Teh, C. Y., & Hay, J. X. W. (2013). Advances in Ultrasound Technology
667 for Environmental Remediation. *SpringerBriefs in Molecular Science*, doi:
668 10.1007/978-94-007-5533-8

669 Xiao, Q., Zhang, J., Xiao, C., Si, Z., & Tan, X. (2008). Solar photocatalytic degradation of
670 Methylene Blue in carbon-doped TiO_2 nanoparticles suspension. *Solar Energy, 82*,
671 706-713.

672 Yang, Y., Wu, Q., Guo, Y., Hu, C., & Wang, E. (2005). Efficient degradation of dye
673 pollutants on nanoporous polyoxotungstate-anatase composite under visible-light
674 irradiation. *Journal of Molecular Catalysis A: Chemical, 225*, 203-212.
675 Zhou, B., Zhao, X., Liu, H., Qu, J., & Huang, C. P. (2010). Visible-light Sensitive cobalt-
676 doped $BiVO_4$ (Co-$BiVO_4$) photocatalytic composites for the degradation of Methylene
677 Blue dye in dilute aqueous solutions. *Applied Catalysis B-Environmental, 99*, 214-221.
678

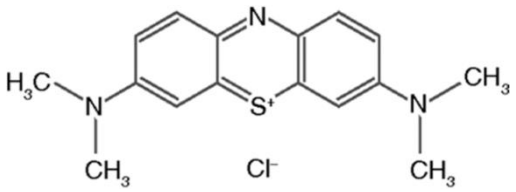

Fig. 1 Molecular structure of methylene blue

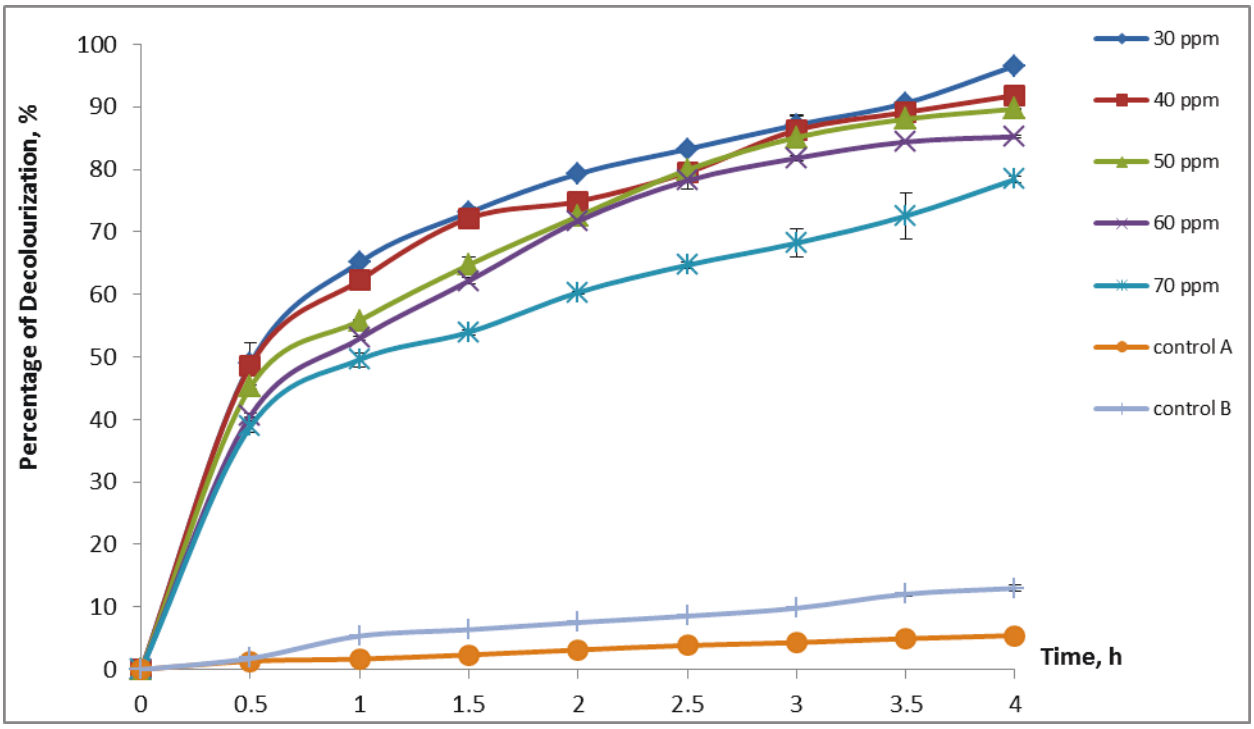

Fig. 2 (a) Effect of initial concentration on the decolourization efficiency of MB; (b) Plot of ln C against time for different initial concentration of MB. The results are averages of triplicate tests. Fixed operating parameters: [TiO_2] = 1.0 g/L; pH = 10.5

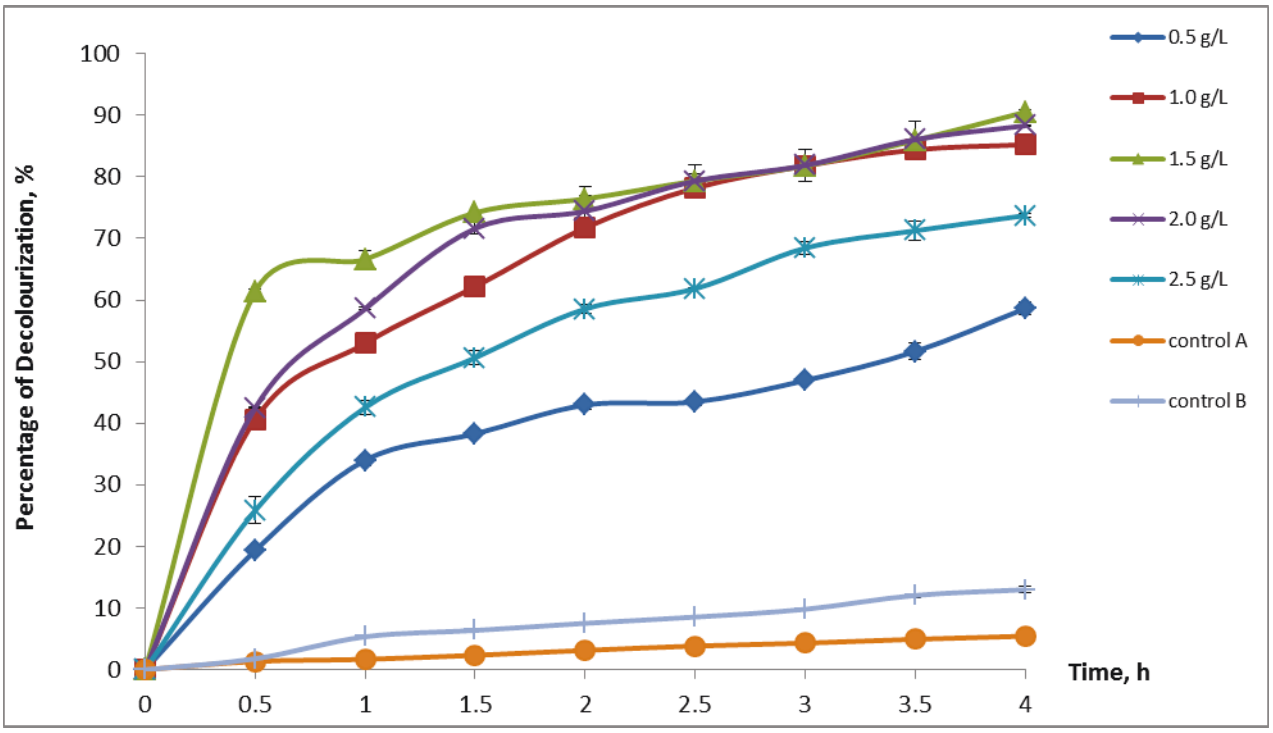

Fig. 3 (a) Effect of catalyst loading on the decolourization efficiency of MB; (b) Plot of ln C against time for different catalyst loading. The results are averages of triplicate tests. Fixed operating parameters: [MB] = 60 ppm; pH = 10.5

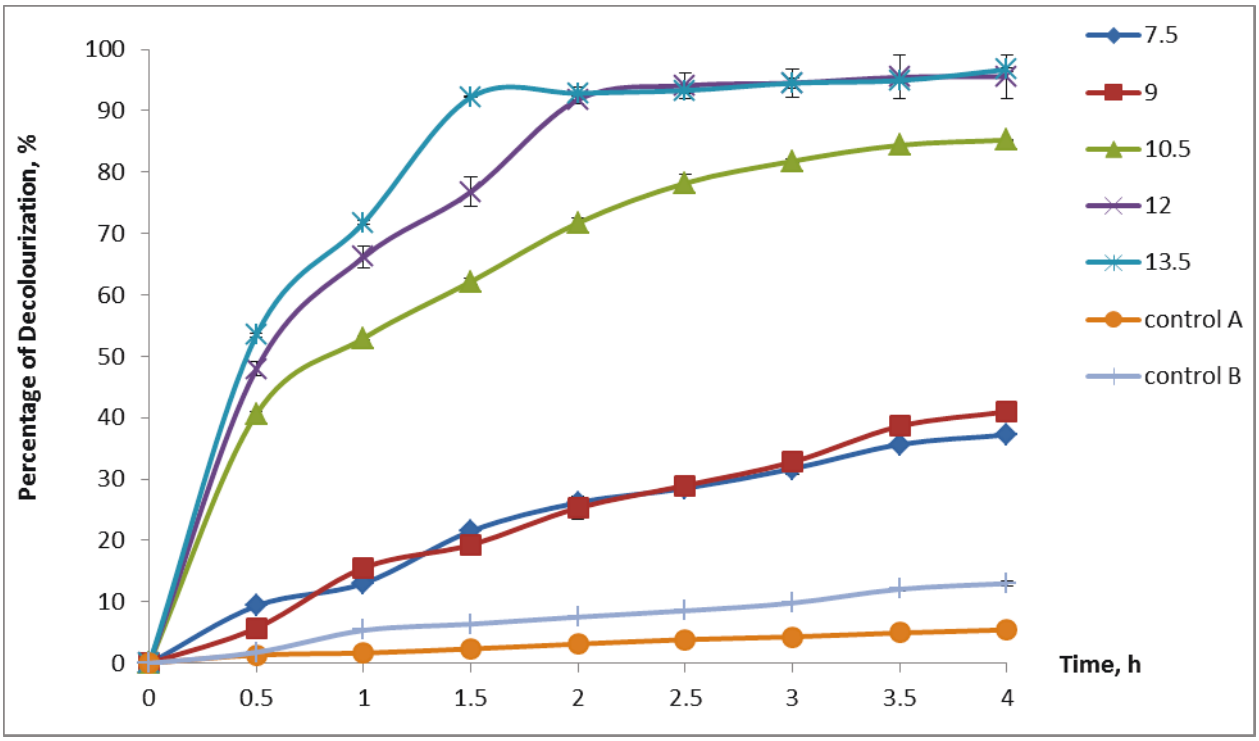

Fig. 4 (a) Effect of initial pH on the decolourization efficiency of MB; (b) Plot of ln C against time for different pH values. The results are averages of triplicate tests. Fixed operating parameters: [MB] = 60 ppm; [TiO_2] = 1.0 g/L

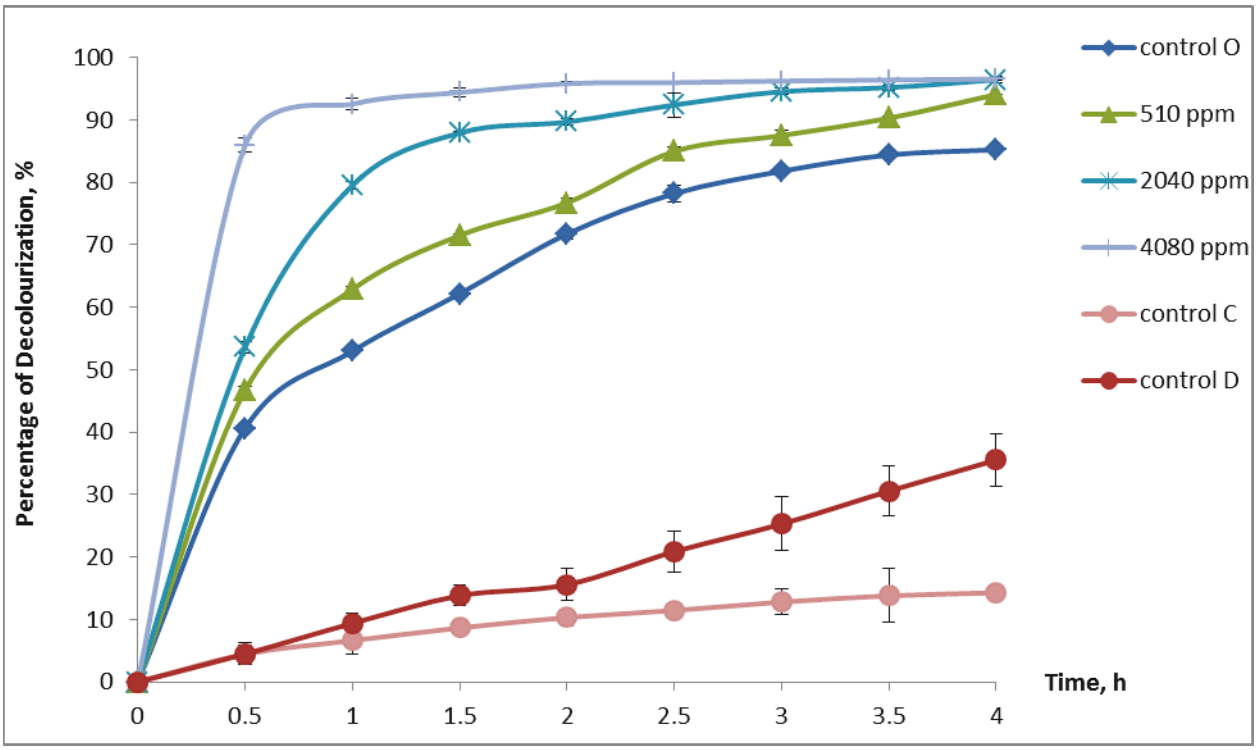

Fig. 5 (a) Effect of H_2O_2 on the decolourization efficiency of MB; (b) Plot of ln C against time for different concentration of H_2O_2. The results are averages of triplicate tests. Fixed operating parameters: [MB] = 60 ppm; [TiO_2] = 1.0 g/L; pH = 10.5

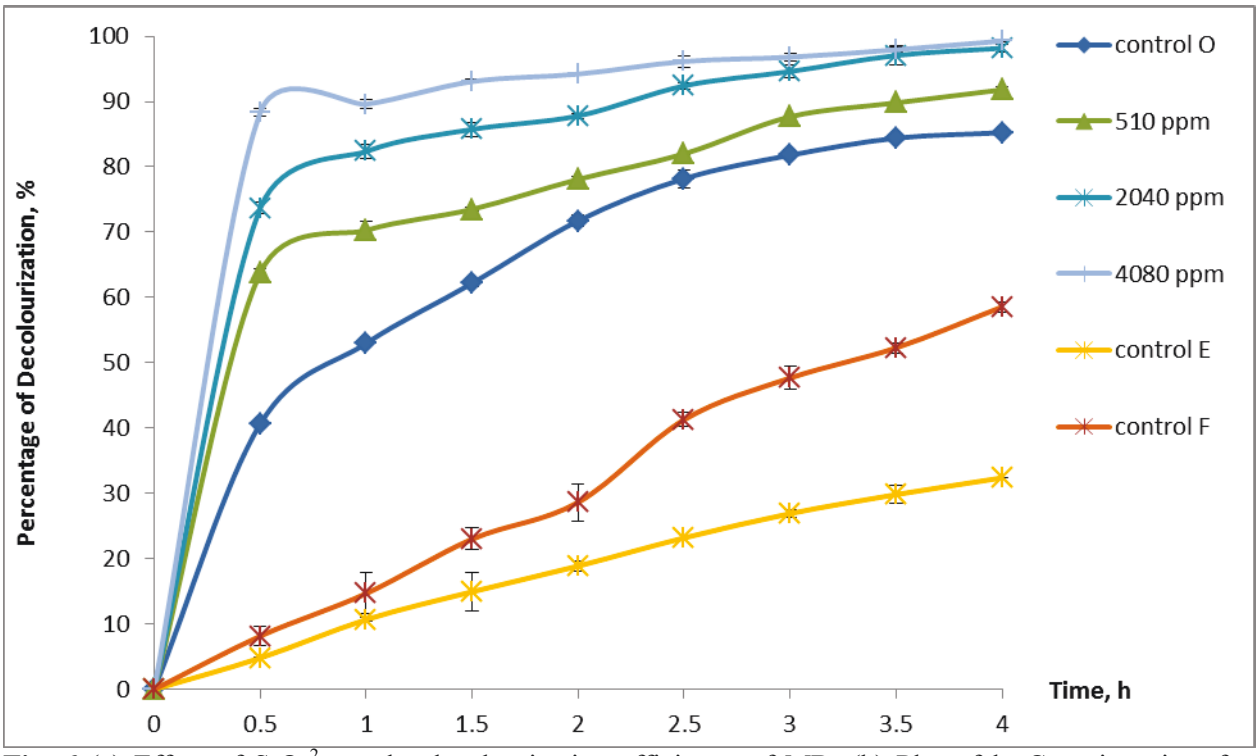

Fig. 6 (a) Effect of $S_2O_8^{2-}$ on the decolourization efficiency of MB; (b) Plot of ln C against time for different concentration of $S_2O_8^{2-}$. The results are averages of triplicate tests. Fixed operating parameters: [MB] = 60 ppm; [TiO_2] = 1.0 g/L; pH = 10.5

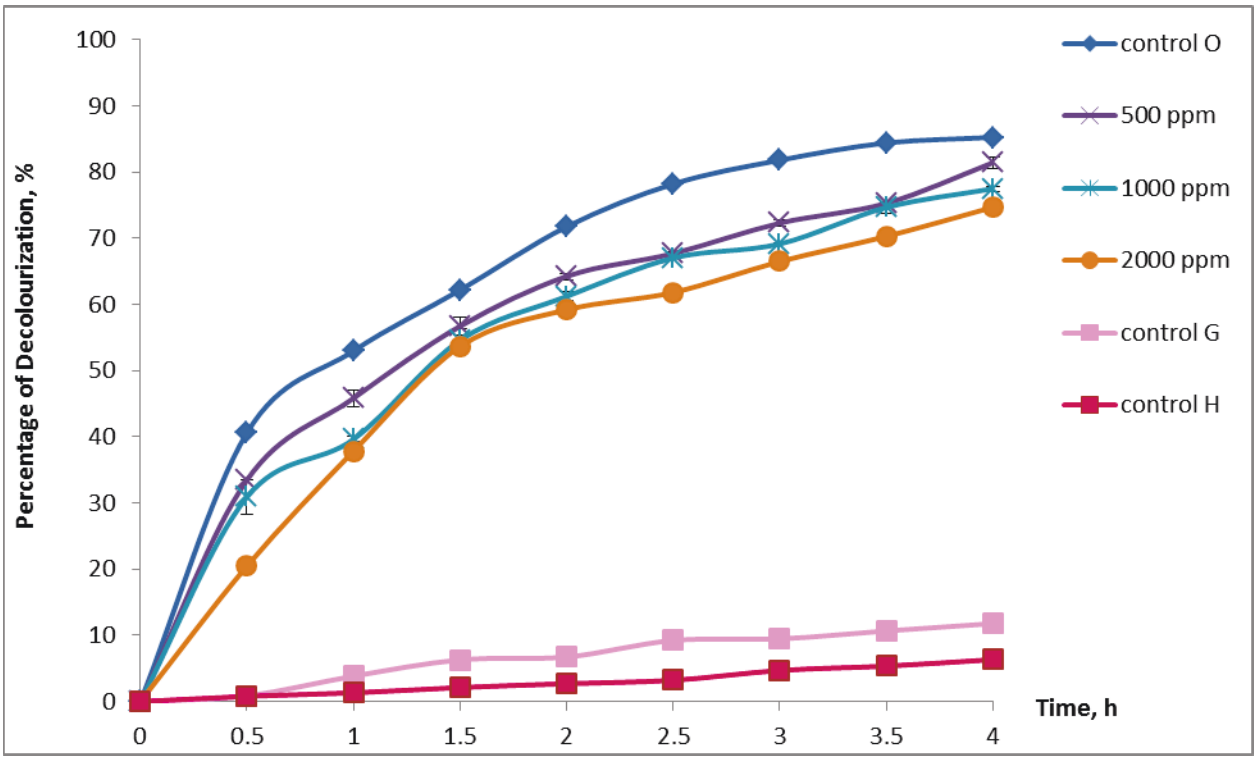

Fig. 7 (a) Effect of Cl^- on the decolourization efficiency of MB; (b) Plot of ln C against time for different concentration of Cl^-. The results are averages of triplicate tests. Fixed operating parameters: [MB] = 60 ppm; [TiO_2] = 1.0 g/L; pH = 10.5

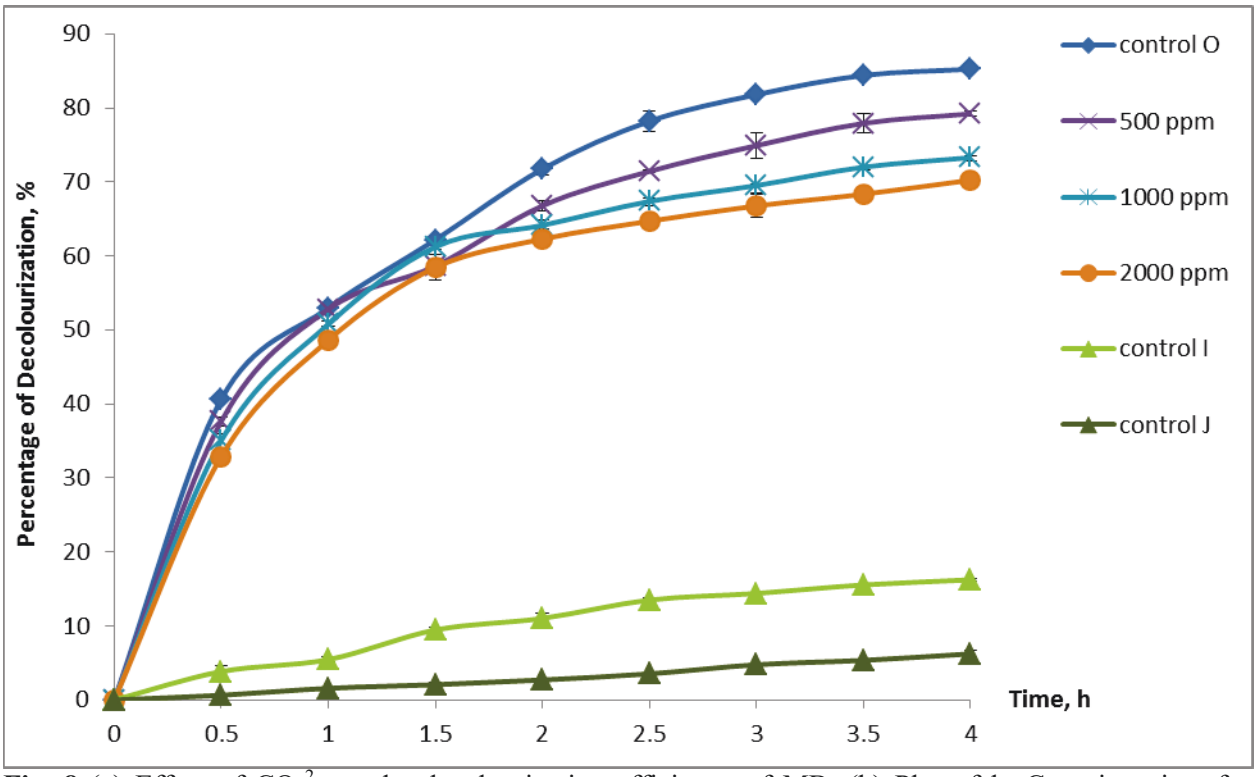

Fig. 8 (a) Effect of CO_3^{2-} on the decolourization efficiency of MB; (b) Plot of ln C against time for different concentration of CO_3^{2-}. The results are averages of triplicate tests. Fixed operating parameters: [MB] = 60 ppm; [TiO_2] = 1.0 g/L; pH = 10.5

Table 1 Experimental operating parameters of each control experimental run

Control	Operating parameters at [MB] = 60 ppm and pH = 10.5
A	Catalysis
B	Photolysis
C	Catalysis; $[H_2O_2]$ = 4080 ppm
D	Photolysis; $[H_2O_2]$ = 4080 ppm
E	Catalysis; $[S_2O_8^{2-}]$ = 4080 ppm
F	Photolysis; $[S_2O_8^{2-}]$ = 4080 ppm
G	Catalysis; $[Cl^-]$ = 2000 ppm
H	Photolysis; $[Cl^-]$ = 2000 ppm
I	Catalysis; $[CO_3^{2-}]$ = 2000 ppm
J	Photolysis; $[CO_3^{2-}]$ = 2000 ppm
O	Photo-catalysis using 1 g/L of TiO_2 without incorporating additives

Catalysis = Experiment conducted in the dark with 1.0 g/L of TiO_2

Photolysis = Experiment conducted under sunlight without any catalyst

Table 2 Pseudo-first-order rate constants, k_{app} for different initial concentration of MB, catalyst loading and initial pH values

Initial concentration of MB, ppm	$10^3 k_{app}$, min^{-1}	Correlation coefficient, R^2
30	18.1	0.976
40	16.1	0.948
50	13.2	0.983
60	10.8	0.945
70	8.23	0.888
Catalyst loading, g/L	$10^3 k_{app}$, min^{-1}	Correlation coefficient, R^2
0.5	4.54	0.767
1.0	10.8	0.945
1.5	12.6	0.817
2.0	11.7	0.936
2.5	7.99	0.892
Initial pH	$10^3 k_{app}$, min^{-1}	Correlation coefficient, R^2
7.5	2.97	0.704
9.0	2.87	0.929
10.5	10.8	0.945
12.0	19.5	0.979
13.5	25.9	0.973

Table 3 Comparison of pseudo-first-order rate constants, k_{app} between different additives

Initial concentration of additive, ppm		$10^3 k_{app}$, min^{-1}	Correlation coefficient, R^2
No additives (control O)		10.8	0.945
H_2O_2	510	14.9	0.973
	2040	26.3	0.965
	4080	66.2	0.988
$S_2O_8^{2-}$	510	14.7	0.890
	2040	56.8	0.969
	4080	91.0	0.999
Cl^-	500	9.2	0.890
	1000	8.4	0.896
	2000	7.8	0.885
CO_3^{2-}	500	9.4	0.885
	1000	8.2	0.876
	2000	7.3	0.845

Experimental conditions: [MB]= 60 ppm, [TiO_2]= 1.0 g/L, pH= 10.5

Table 4 Comparison of pseudo-first-order rate constants, k_{app} for decolourization of MB using TiO_2 between present and previous studies

Initial Concentration of MB, ppm	$10^3 k_{app}$, min^{-1}	Experimental Conditions	Reference
60 (without any additive) 60 (with 4080 ppm $S_2O_8^{2-}$)	10.8 91.0	$[TiO_2]$= 1.0 g/L Initial pH=10.5 Irradiation= sunlight Irradiation time= 240 min	Present study
27	53.0	$[TiO_2]$= 0.5 g/L pH= 7 Irradiation= UV light Irradiation time= 200 min	Lachheb et al., 2002
3	67	$[TiO_2]$= 0.25 g/L Initial pH= 3 Irradiation= UV light Irradiation time= 60 min	Lee et al., 1999
23	60	$[TiO_2]$= 2.5 g/L pH= 6 Irradiation= UV light Irradiation time= 90 min	Houas et al., 2001
10	29.3	$[TiO_2]$= 2.0 g/L Initial pH= unspecified Irradiation= visible light Irradiation time= 600 min	Lin et al., 2007
6	45.4	$[TiO_2]$= 0.7 g/L Initial pH=4.3 Irradiation= UV light Irradiation time= 80 min	Chen et al., 2003
15	67.2	$[TiO_2]$= 1.2 g/L Initial pH= unspecified Irradiation= UV light Irradiation time= 30 min	Li and Li, 2002